JOURNAL OF CATALYSIS 145, 437–449 (1994)

Deactivation of Steam-Reforming Model Catalysts by Coke Formation

II. Promotion with Potassium and Effect of Water

Mario C. Demicheli,* D. Duprez,*,[1] J Barbier,* O. A. Ferretti,† and E. N. Ponzi†

*Laboratoire de Catalyse en Chimie Organique, URA CNRS 350, Université de Poitiers, 40 Avenue du Recteur Pineau, 86022 Poitiers Cedex, France, and †Centro de Investigacion y Desarrollo en Procesos Catalíticos, Calle 57 No. 257, La Plata, Argentina

Received February 1, 1993; revised July 12, 1993

The influence of potassium on the hydrogenolysis of cyclopentane and on the simultaneous carbon formation over a series of alumina-supported Ni catalysts was studied. With increasing potassium loadings at temperatures where either a deactivating two-dimensional carbon or a filamentary carbon was formed, the catalytic activity passed through a maximum and then decreased. With relatively high K-doses there was less coking in the presence of steam; the growth of filamentary carbon was then largely reduced. Characterization of the coked catalysts by temperature-programmed oxidation and SEM disclosed quite different roles of alkali: at lower contents, associated with alumina, potassium facilitates the formation of filamentary carbon and minimizes the generation of coke precursors, whereas at higher contents it acts as a poison for both hydrogenolysis and coking reactions. In all cases, the alkali promoted the catalytic oxidation of the carbon deposits. Because of its localization, the alkali could also modify the nickel–carbon interface in carbon filaments. © 1994 Academic Press, Inc.

INTRODUCTION

In many industrial processes, the addition of small amounts of alkali ions (0.5–1%) to metal-supported catalysts has a strong influence on their catalytic properties and lifetimes. However, in other processes (hydrogenation, steam-reforming, methanation, etc.), larger amounts of alkali have to be added to reduce carbon deposition and stabilize the catalyst (1, 2), which is often detrimental to the catalytic activity of the reaction. Thus, 2–10% potassium is added to Ni catalysts used in steam-reforming of naphthas (2) and to styrene catalysts (3).

Concerning the effect of alkali on the formation of carbon species, Figueiredo and Trimm (4) have reported that the presence of potassium in the support does not affect the specific rate of filament formation from propane on nickel. To the contrary, Chen and Chen (5) have recently observed that alkali ions decrease the coking rate of Ni/Al_2O_3 catalysts during the cracking of *n*-hexane. Potassium is not likely to promote the gasification by hydrogen of carbon formed on supported nickel (6). However, during gasification by water, the promoting action of potassium is weakened by hydrogen (7).

In Part I of this work (8), we established the main variables affecting the kinetics of carbon formation in the hydrogenolysis of cyclopentane on alumina-supported nickel catalysts. In this second part, the effect of potassium addition (as K+ ions) to Ni/Al_2O_3 catalysts on the hydrogenolysis of cyclopentane and on coke deposition have been investigated. Particular attention was paid to the study of the different carbon morphologies induced by the added alkali. Finally, the influence of water was analyzed using a K-rich catalyst.

EXPERIMENTAL

Catalyst Preparation

Catalysts were prepared by successive impregnation of nickel and potassium. 80 g of a Rhône Poulenc δ-Al_2O_3 (particle size = 0.1–0.2 mm, referred to as AC) was immersed into 130 ml (three times the pore volume) of a $Ni(NO_3)_2 \cdot 6H_2O$ (Fluka) solution of the appropriate concentration to obtain ~ 10% Ni in the final catalysts. The resulting slurry was dried at 80°C under continuous stirring, then at 120°C overnight, and finally heated in flowing air (1°C min^{-1}) to 350°C and maintained at that temperature for 10 h. This solid is designated Ni10AC. The solid was subsequently reimpregnated with different amounts of a 2-*M* solution of K_2CO_3 (Normapur), dried as indicated, and heated in flowing air to 400°C. The catalysts are referred to as Ni10KYAC, with Y being a limiting value of the potassium content. In order to generate interactions between the components, some parts of

[1] To whom correspondence should be addressed.

0021-9517/94 $6.00

TABLE 1

Elemental Analysis and BET Surface Area of the Calcined Catalysts

Catalyst	Elemental control (%)			K/Ni atomic ratio	Surface area ($m^2\ g^{-1}$)
	Ni	K	C		
Ni10AC	8.81	<0.01	0	0	75
Ni10K0.6AC	9.40	0.57	<0.1	0.091	—
Ni10K1AC	9.31	0.99	0.19	0.16	—
Ni10K2AC	9.27	1.83	0.27	0.30	—
Ni10K4AC	8.45	4.29	0.64	0.76	62
Ni10K5AC	8.63	5.22	0.62	0.91	—
Ni10AC700	9.02	<0.01	0	0	49
Ni10K4AC700	8.67	4.26	0.02	0.74	57

Ni10AC and Ni10K4AC were calcined in static air at 700°C for 18 h. These catalysts were differentiated by the postfix 700. Alkali and nickel contents were determined by atomic absorption spectrophotometry, whereas carbon was dosed chromatographically after being oxidized under flowing oxygen at 1050°C. The resulting values are listed in Table 1. K and Ni contents of the freshly reduced and passivated catalysts corresponded well to those of their oxide states. In contrast, only traces of carbon were detected, which proves that the potassium carbonate remaining after calcination at 400°C is fully hydrolyzed during reduction (2, 3).

Activation and Coking Reaction

When the reaction was carried out in a dry atmosphere, a one-inlet flow reactor was used, whose characteristics were detailed in Part I (8). In the experiments with steam, a second inlet branch was added to feed the reactor with a constant steam flow. Deionized water was used to generate steam in an evaporator fed by a motor-driven syringe (Braun). The three reactants (cyclopentane, hydrogen, and steam) were mixed at the top of the reactor before flowing down through the catalyst bed. Prior to reaction, the catalyst was heated at 1°C min^{-1} in flowing hydrogen to 500°C, and allowed to remain at that temperature for 10 h. Then it was cooled to the reaction temperature under the H_2/H_2O mixture. The reaction was started by admitting cyclopentane together with this mixture. After the reaction, cyclopentane and steam were switched off and the catalyst was quenched to room temperature under the remaining hydrogen. In all cases the catalysts were passivated with a mixture of 1% O_2 in nitrogen at room temperature before being removed from the reactor. The effluent was analyzed by combining one FID and two TCD gas chromatographs. An Al_2O_3–KCl capillary column with hydrogen as carrier gas was used to analyze light hydrocarbons in the FID; a Porapak-Q packed column with hydrogen as carrier gas was used to analyze CO and CO_2 in one of the TCD's; and a 5A molecular sieve packed column with nitrogen as carrier gas was used to analyze hydrogen in the other TCD.

Dispersion Measurements

Metal surface and metal reduction parameters were determined using a pulse chromatographic system described elsewhere (9). The catalyst was reduced at 500°C (same procedure as for reaction) and then purged in flowing argon at 500°C for 3 h. After cooling to room temperature, pulses of hydrogen (0.245 ml) were admitted every minute, until saturation. The resulting hydrogen uptake, H_C^T, includes both reversibly and irreversibly adsorbed hydrogen. The interruption of H_2 injection for 10 min made part of the hydrogen desorb, and this quantity, H_C^R, was used to estimate the amount of reversibly adsorbed hydrogen. The next step was the hydrogen thermodesorption at 10°C min^{-1} up to 500°C. At that temperature the oxygen uptake, O_C^{500}, was measured (by sending oxygen pulses every minute) to evaluate the amount of reduced nickel, Ni_R, and the reduction degree $R_c = 100\ Ni_R/Ni$ (8).

Temperature-Programmed Oxidation

The reactivity of the deposited carbon species was studied by temperature programmed oxidation under a flow of 2% O_2 in helium at 7°C min^{-1}. A pulse chromatographic system with a Porapak-Q column was used for separating excess oxygen from the CO_2 formed (10).

Electron Microscopy and Spectroscopy

Samples of coked catalysts were ultrasonically dispersed in ethanol, and a drop of the slurry was deposited on a carbon-coated copper grid. Specimens containing potassium were prepared by sedimentation on a grid of an aerosol produced by a shock wave in a glass tube

containing the powdered sample (11). The local composition was determined by energy-dispersive X-ray emission spectroscopy (EDX) associated with a scanning transmission electron microscope (STEM) equipped with a field-emission gun (Vacuum Generators VGHB501). Examination of coked catalysts by SEM was performed in a JEOL 35 CF electron microscope.

RESULTS

Characterization of Fresh Catalysts

Table 2 shows that the total amount of hydrogen chemisorbed, H_C^T, increases with potassium loading for the catalysts calcined at 400°C. The reversibly adsorbed hydrogen, H_C^R, followed the same tendency, and was estimated to be 4–5% of the total for each catalyst. However, the oxygen uptake, O_C^{500} (Table 2), was proportional to the nickel content of the catalysts, and a reduction degree of virtually 100% was attained with all calcined catalysts at 400°C (a constant stoichiometry $O/Ni_R = 1.1$ was assumed (8)). On the other hand, blank experiments performed with pure or alkalized alumina gave only a small reversibly adsorbed hydrogen uptake. It follows from these measurements that the metal dispersion D_C, which is proportional to H_C/O_C^{500} (8), increases with potassium content (Table 2).

Effect of Potassium on Hydrogenolysis and Coking from Cyclopentane

In Part I (8) it was shown for a 10% Ni/Al_2O_3 catalyst that within a region of relatively low temperature ($T < T_B$) the carbon deposited is very toxic for the metallic function (deactivating two-dimensional carbon). On the other hand, at temperatures higher than T_B (8), the thermodynamic conditions become favorable for carbon nucleation at the rear of the nickel crystallites, and carbon filaments appear on the catalyst surface.

The reaction of cyclopentane (CPA) with hydrogen was carried out at 420 and 460°C at a molar ratio H_2/CPA = 1.75, to form the deactivating two-dimensional carbon and the filamentary carbon, respectively. In Fig. 1, the amounts of carbon deposited after a 1-hour reaction at 420°C and a 0.5-hour reaction at 460°C are plotted as a function of the initial K/Ni ratio. For the two domains of carbon formation, viz., two-dimensional and filamentary, the maxima of carbon deposition appear for a K/Ni value of 0.3. The changes in the activity for carbon deposition at 420°C (Table 3) and at 460°C (Table 4) are accompanied by parallel, though less marked, changes in activity for hydrogenolysis. The activity maxima for the hydrogenolysis reactions are obtained for a slightly lower K content. Both high temperatures and the presence of potassium enhanced hydrogenolysis to yield essentially methane as gaseous product ($C_2/C_1 < 10^{-2}$). With the unpromoted catalysts, cycloolefins were detected in small quantities at the beginning of the reaction, and all catalysts gave some aromatization at low temperature. With regard to the stability of the catalysts, a maximum

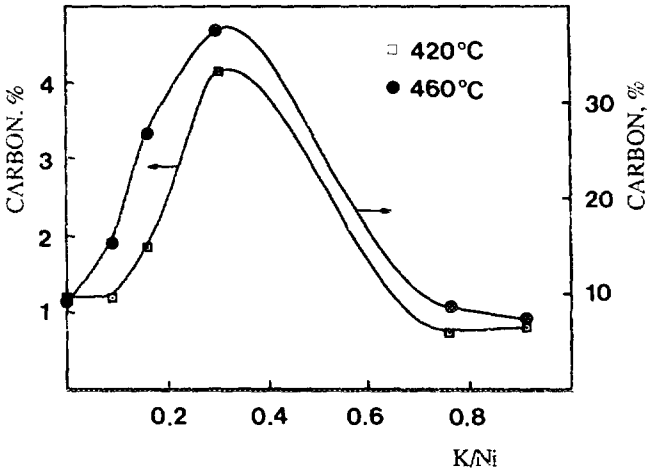

FIG. 1. Variation of the amount of carbon deposited with the K/Ni ratio for Ni–K/Al_2O_3 catalysts. H_2/CPA = 1.75; reaction times 1 h at 420°C and 0.5 h at 460°C.

TABLE 2

Metal Surface Parameters of the Reduced Catalysts at 500°C

Catalyst	H_C^T 10^3 mol g^{-1}	O_C^{500} 10^3 mol g^{-1}	Reduction degree R_C (%)	Dispersion D_C (%)
Ni10AC	0.128	1.58	95	18
Ni10K0.6AC	0.141	1.78	100	18
Ni10K1AC	0.151	1.75	99	19
Ni10K2AC	0.172	1.74	99	22
Ni10K4AC	0.194	1.50	94	29
Ni10AC700	0.018	0.73	37	5.5
Ni10K4AC700	0.014	0.59	36	5.3

TABLE 3

Activities and Selectivities for Coking and Hydrogenolysis of the K-Containing Catalyst

Catalyst	Global activity 10^3 mol h^{-1} g^{-1}	%C	Partial activity		Selectivity	
			Coking	Hydrog.	Coking	Hydrog.
Ni10AC	53.7	1.18	0.65	53.0	1.21	98.8
Ni10K0.6AC	57.3	1.20	0.67	52.6	1.17	98.8
Ni10K1AC	68.2	1.85	1.03	67.2	1.51	98.5
Ni10K2AC	59.8	4.16	2.31	57.5	3.86	96.1
Ni10K4AC	60.3	0.74	0.41	59.9	0.68	99.3
Ni10K5AC	64.7	0.79	0.44	64.3	0.68	99.3

Note. T = 420°C, H_2/CPA = 1.75; reaction time = 1 h.

loss of 20% potassium was observed with Ni10K5AC after a half-hour reaction at 460°C.

Reactivity of the Coked Catalysts with Oxygen

Samples of the coked catalysts were characterized by temperature programmed oxidation up to 900°C. Figure 2 gives the amount of CO_2 evolved from the catalysts on which the CPA+H_2 reaction was undertaken at 420°C. Despite the complexity due to partial superimposition of the peaks, there are some clear and informative features. At low potassium content, the carbon formed is very reactive: its oxidation starts at about 100°C, and the maximal rate of consumption occurs at 380–420°C (curves a and b). Increasing the potassium loading leads to the organization of the carbon deposit, and less reactive species arise at 480 and 540°C (curve c for Ni10K2AC). For a K/Ni ratio higher than 0.8 there is a significant change in the TPO profile of coke, i.e., the carbon oxidizable at low temperature disappears as well as the less reactive deposit. The remaining small carbon laydown is fully oxidized at 380°C. The slow evolution of CO_2 over 710°C, which takes place without oxygen consumption, accounts for the decomposition of very refractory potassium carbonate. It is interesting to compare the TPO-profile given by Ni10AC with that of Ni10K2AC, both coked under the same conditions (Fig. 3). On Ni10K2AC, after 1 h reaction, there are different carbon types on the surface (curve c), whereas Ni10AC gives rise to a unique species (curve b) oxidizable at 380°C, even after several hours of reaction.

The TPO profiles corresponding to the catalysts coked at 460°C (Fig. 4) show that (i) as the K/Ni ratio increases together with the amount of carbon deposit, new intermediate carbon species develop, and (ii) the major peak attributed to filamentary carbon moves to lower temperatures on K addition, and this regardless of its size. Here again, the flat peak at high temperature resulting from the decomposition of surface potassium carbonate appears for catalysts with high potassium doses. Thus, the formation of this phase might not be favored under fast filament growing or combustion rates. In Fig. 4 (insert) the maximum temperature (T_m) of the main peak was plotted as a function of the K/Ni ratio. It is seen that the promoting action is stronger at higher K content. As confirmed by SEM, all these catalysts formed carbon filaments. Estimations of the global H/C ratio of the carbonaceous deposits were made for some catalysts. H/C ratios of 0.5

TABLE 4

Activities and Selectivities for Coking and Hydrogenolysis of the K-Containing Catalyst

Catalyst	Global activity 10^3 mol h^{-1} g^{-1}	%C	Partial activity		Selectivity	
			Coking	Hydrog.	Coking	Hydrog.
Ni10AC	119	8.9	9.9	109	8.3	91.7
Ni10K0.6AC	148	15.3	17	131	11.5	88.5
Ni10K1AC	310	26.8	30	280	9.6	90.4
Ni10K2AC	198	37.4	42	156	21.0	79.0
Ni10K4AC	89	8.9	9.9	79	11.1	88.9
Ni10K5AC	174	7.2	8.0	166	4.6	95.4

Note. T = 460°C, H_2/CPA = 1.75; reaction time = 0.5 h.

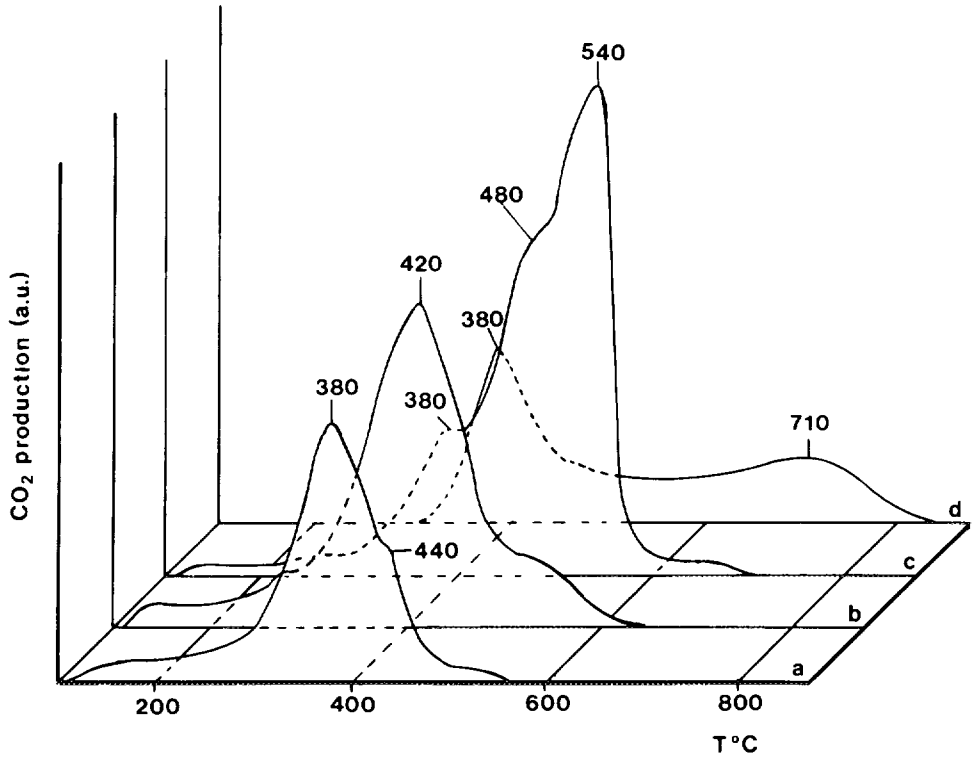

FIG. 2. TPO profiles of the coked catalysts at 420°C. (a) Ni10K0.6AC, (b) Ni10K1AC, (c) Ni10K2AC, (d) Ni10K4AC.

and 1, respectively, were obtained for Ni10AC and Ni-10K5AC, after being coked at 420°C. By contrast, the resulting values for the deposits formed at 460°C were, for all catalysts, very close to 0.

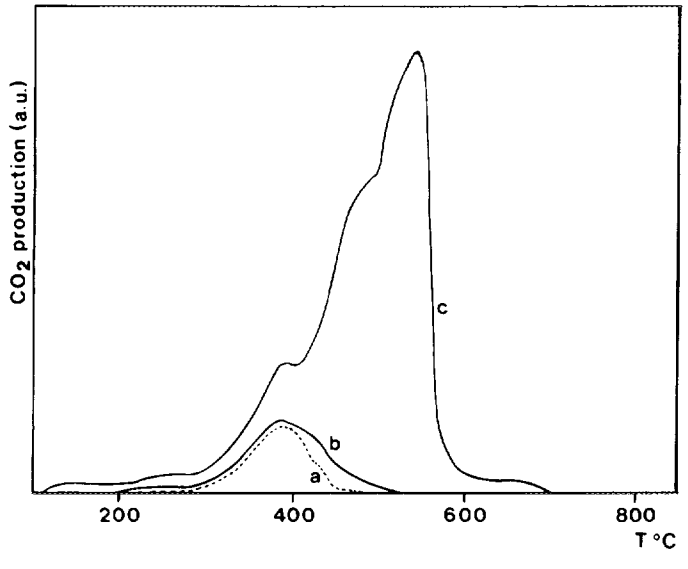

FIG. 3. TPO profiles of the coked catalysts at 420°C (H_2/CPA = 1.75): Ni10AC after (a) 1 h reaction, (b) 4 h reaction; Ni10K2AC after (c) 1 h reaction.

Characterization of Coked Catalyst. Localization of Potassium in Carbon Filaments Produced by Nickel

It was previously reported both for unpromoted (8) and K-promoted Ni/Al_2O_3 catalysts (12) that, upon carbon filament growth, catalytic activities for hydrogenolysis and hydrogenation reactions are partially recovered. In contrast, the bidimensional deposit formed at low temperatures (380–430°C for H_2/CPA=1.75) leads to a continuous decay of the activity. Of all the catalysts on which the reaction had taken place at 420°C, only Ni10K2AC displayed carbon filaments on the surface, as seen in Fig. 5. Instead of "true" filaments, i.e., hollow graphitic fibers with a pear-shaped nickel cluster at the tip (13), thin threads of about 20 nm in diameter, consisting presumably of amorphous carbon (13, 14) are observed. These morphologies are quite compatible with the variety of carbon states visualized in the TPO patterns (Fig. 2), and have never been observed with K-free catalysts. It was generally reported that a minimum nickel crystal diameter of about 10 nm is needed for nucleation of a carbon filament, and therefore smaller crystallites remain on the surface, encapsulated by carbon (13–15). However, even for every short reaction times, the mean diameter of filaments grown on unpromoted catalysts was around 50 nm. Consequently, we believe that an extra amount of potassium, nonassociated with

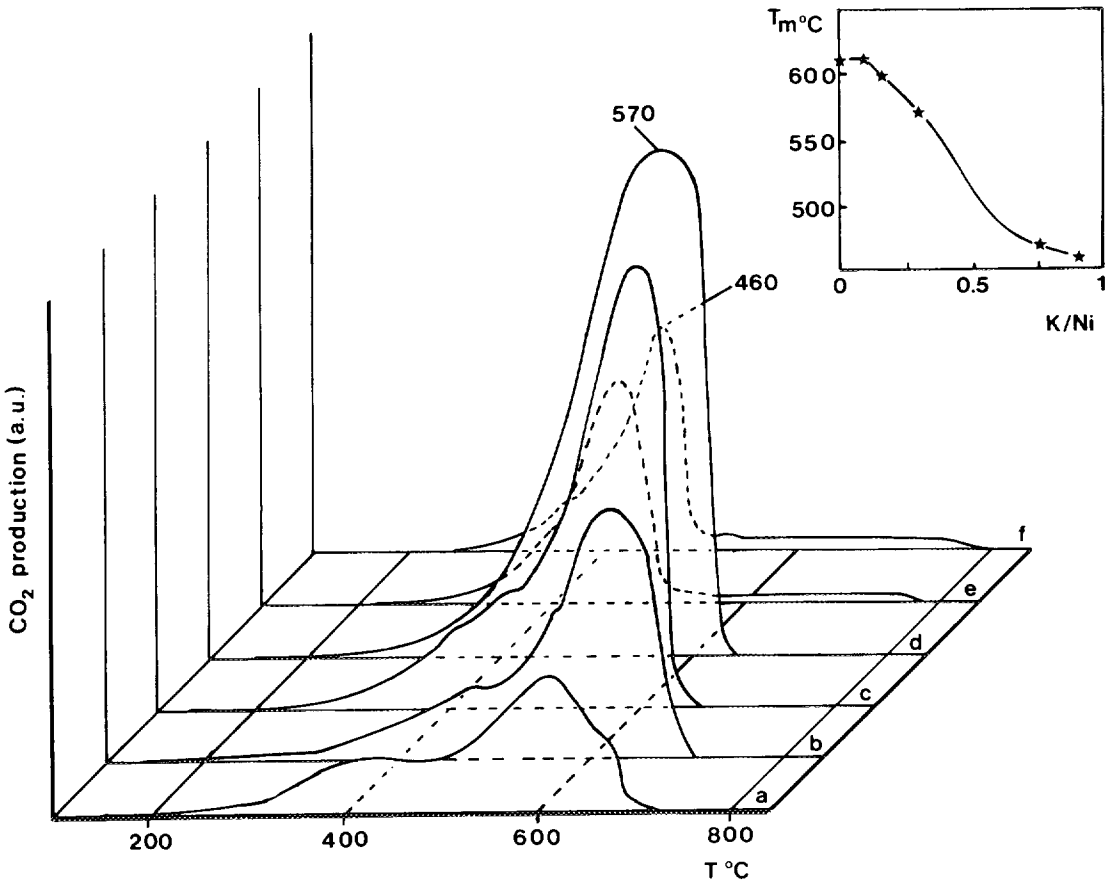

FIG. 4. TPO profiles of the coked catalysts at 460°C: (a) Ni10AC, (b) Ni10K0.6AC, (c) Ni10K1AC, (d) Ni10K2AC, (e) Ni10K4AC, (f) Ni10K5AC. Inset: temperature of the rate maximum for the main CO_2 peak versus the K/Ni ratio.

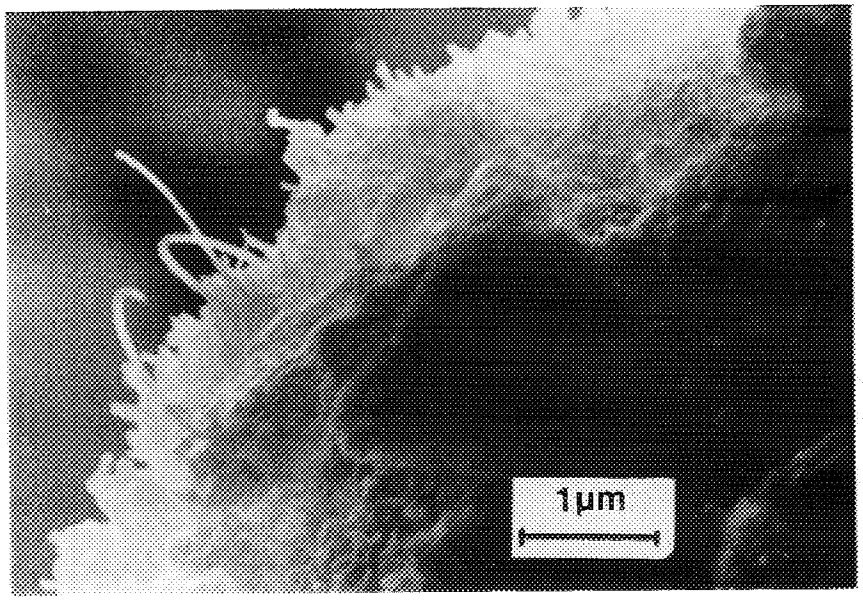

FIG. 5. Ni10K2AC coked at 420°C, H_2/CPA = 1.75, reaction time 1h.

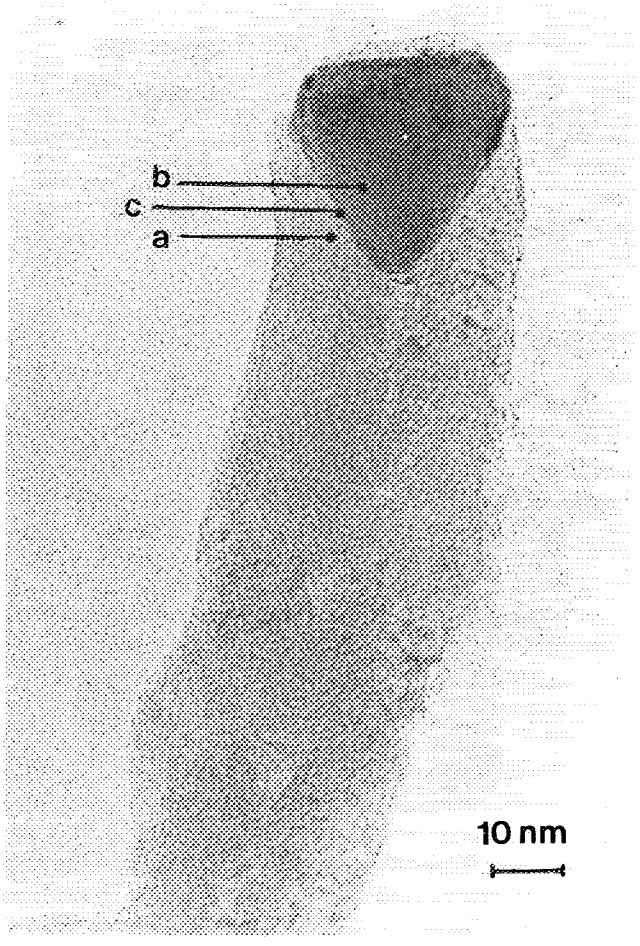

FIG. 6. Carbon filament formed on Ni10K4AC at 460°C showing the zones of the EDX analysis.

alumina, may affect smaller nickel crystallites and render them more easily detachable from the surface, so that they can give rise to thin carbon filaments. Supporting this claim is the high temperature peak at 540°C observed in Fig. 3 for Ni10K2AC (curve c) which is associated with that carbon species.

A STEM—EDX analysis was performed throughout a carbon filament formed at 460°C on Ni10K4AC (Fig. 6), with the aim of detecting potassium. In Fig. 7, spectrum (a), taken on carbon in the vicinity of the nickel particle, or spectrum (b), on the exposed nickel surface, does not show any traces of potassium, whereas spectrum (c), taken at the interface between nickel and carbon, reveals the presence of potassium. This particular localization of

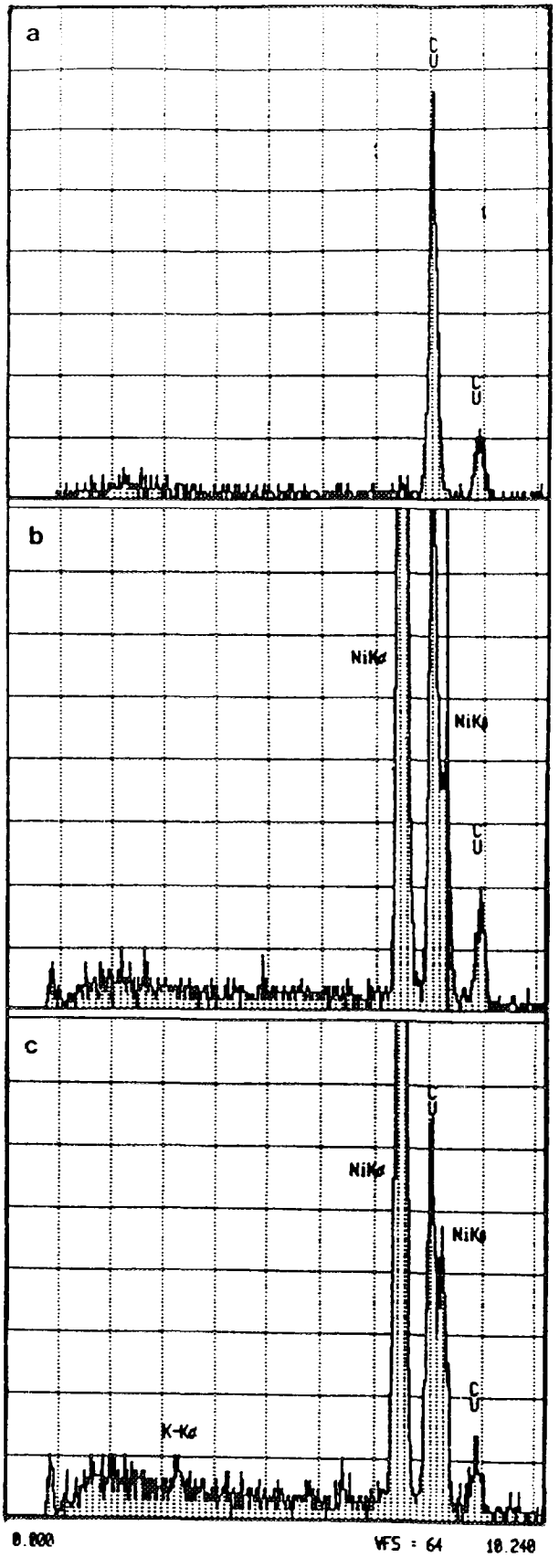

FIG. 7. EDX spectra resulting from analysis performed on the filament of Fig. 6: (a) carbon in the vicinity of the nickel particle, (b) exposed nickel surface, (c) interface between nickel and carbon.

the alkali could affect the covalent bonds between the nickel faces (probably Ni(111) and Ni(311) (16)) and the basal planes of graphite, thus lowering the adhesion strength of the particle. In fact, with carbon deposits formed on highly loaded potassium catalysts, it is very frequent to observe carbon filaments which have lost their nickel particles (17).

K-Rich Ni/Al_2O_3 Catalysts. Effect of Water

Figure 8 shows that Ni10K4AC gives less carbon in the whole temperature range and, as with the unpromoted catalysts, an abrupt change in the apparent activation energy (breakpoint B) is revealed. The catalysts calcined at 700°C were compared in a similar manner, and the data are plotted in Fig. 9. In this case, also, potassium appears to reduce the coking rate, although this trend is reversed at temperatures below 420°C. Because each pair of catalysts, promoted and unpromoted, should have similar particle sizes, it follows that the growing of filamentary carbon on K-containing catalysts sets in at a lower C/Ni_s ratio than in K-free catalysts. This could be explained by an intimate contact between K ions and Ni particles existing at relatively high K contents. Figure 10 (a and b) shows the SEM micrographs obtained with catalysts coked at 460°C, under net growing of filamentary carbon. A lower filament density (number of filaments per unit surface area) is observed for the catalyst with 4% K (Fig. 10b) than for the unpromoted catalyst (Fig. 10a), in agreement with the lower coking rate of the former (Fig. 9). In addition to filaments, acicular graphite fibers grew abundantly on the unpromoted catalysts (Fig. 10-a). It is possible that these fibers were extruded from nickel particles in strong interaction with the alumina (13). Hence, the presence of potassium appears to weaken such interactions.

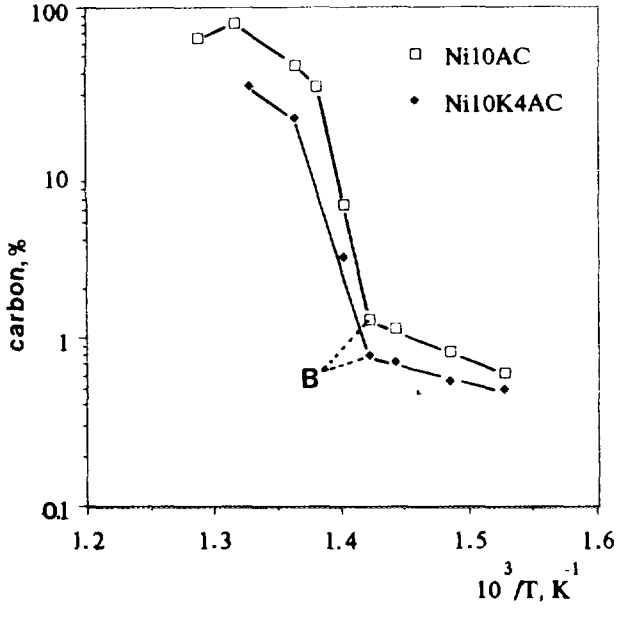

FIG. 8. Temperature dependence of coke deposition from CPA/H_2 mixtures on K-rich catalysts calcined at 400°C. P_{CPA} = 36 kPa, P_{H_2} = 64 kPa.

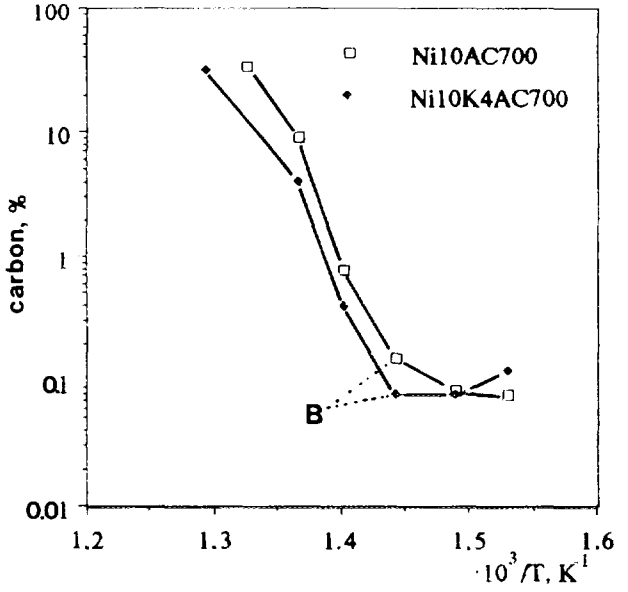

FIG. 9. Temperature dependence of coke deposition from CPA/H_2 mixtures on K-rich catalysts calcined at 700°C. P_{CPA} = 36 kPa, P_{H_2} = 64 kPa.

The effect of water was studied comparatively on Ni10AC and Ni10K4AC. A ratio of H_2, H_2O, and CPA of 1.75:1.04:1 was maintained to have carbon deposition over the entire temperature range. Identical runs were carried out by replacing steam by the same partial pressure of nitrogen. Figure 11 shows that water causes a slight decrease of the coking rate on Ni10AC, only at low temperatures. Carbon filaments started growing immediately after the B-point at a rate not affected by water. In turn, Fig. 12 shows for Ni10K4AC a quite different behavior when water is present: as the temperature increases from 400°C the coking rate decreases, goes through a flat minimum, and then rises progressively. In this case, the absence of such an abrupt change in slope is the result of a high promotion by the alkali of the catalytic gasification of filamentary carbon by water, in line with the small amount of this carbon type observed by SEM. The gaseous products were mainly CH_4, CO, and CO_2, with a distribution of higher hydrocarbons very similar to the one obtained in the absence of water. Neither light olefins nor oxygenated products were detected with any of the catalysts. This led us to calculate mean values of

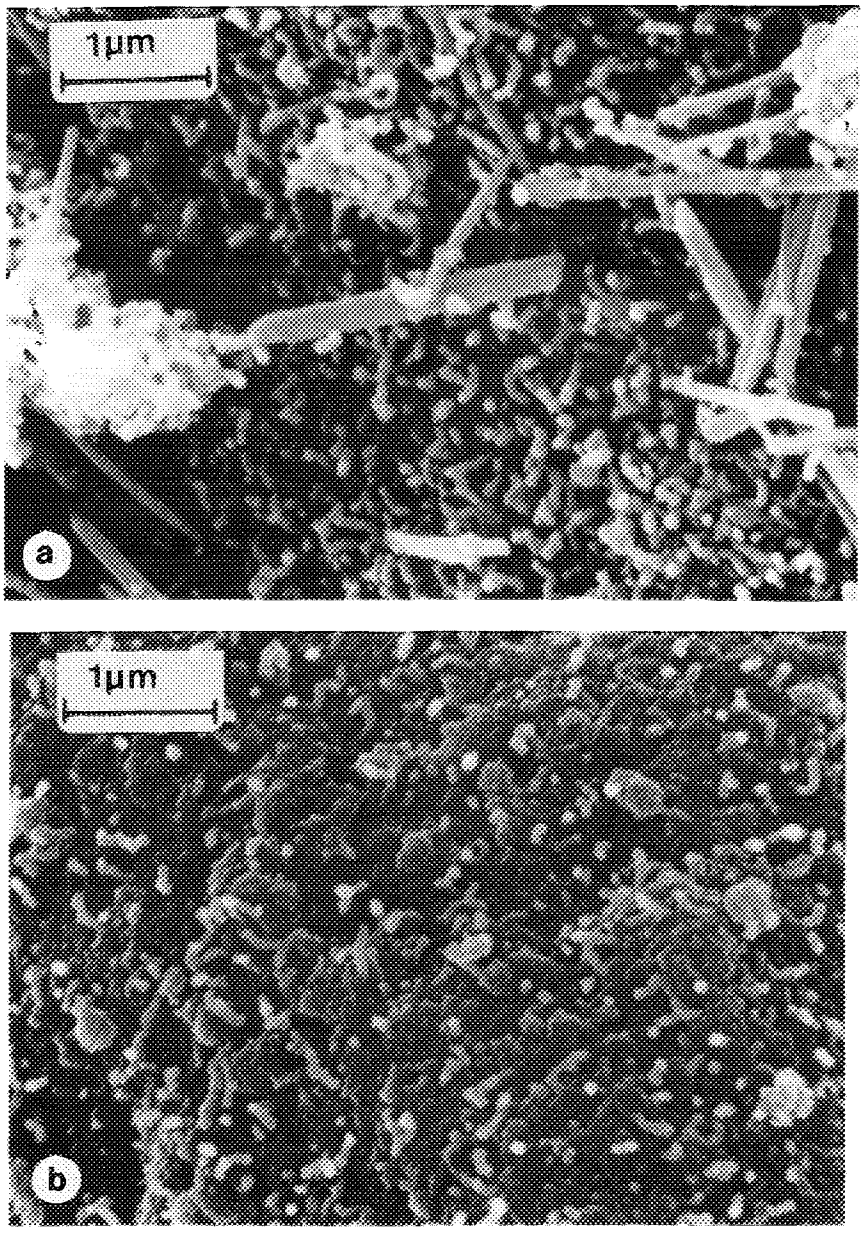

FIG. 10. (a) Ni10AC700 coked at 460°C; H_2/CPA = 1.75; reaction time = 0.5 h. (b) Ni10K4AC700 coked at 460°C; H_2/CPA = 1.75; reaction time = 0.5 h.

product selectivities, $\langle S_i \rangle$, defined as

$$\langle S_i \rangle = \frac{\text{moles of CPA transformed into } (i)}{\text{moles of CPA converted}}$$

with index i being H for hydrocarbons, O for CO + CO_2, and C for carbon (coke).

In Table 5, the most relevant values of conversion and selectivities are given. At lower temperatures, the virtual absence of deactivating carbon on Ni10K4AC makes this catalyst display a higher activity compared to its unpromoted homologues. At 500°C, however, full conversion is attained with Ni10AC, but mostly because of the heavy production of carbon filaments.

Complementary work has shown that the increase in the selectivity to carbon oxides observed with Ni-10K4AC is due to a greater inhibition by potassium of hydrogen than of steam reactions. Moreover, as the methanation reaction on promoted catalysts is more severely inhibited than the water-gas shift reaction, the to-

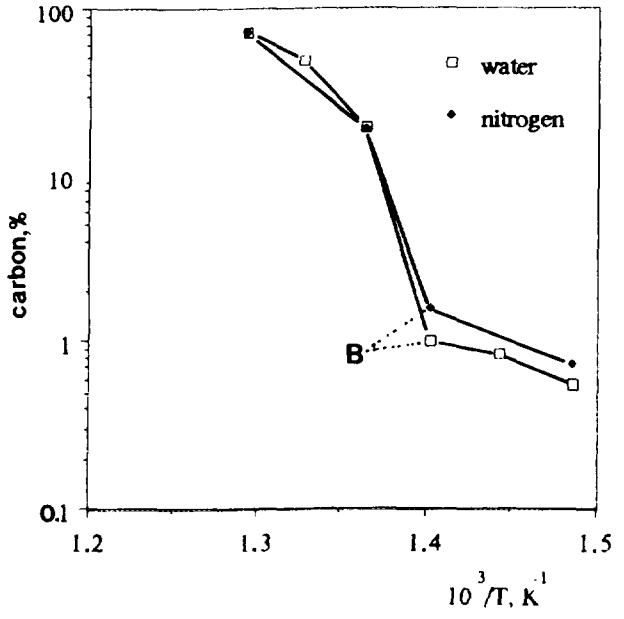

FIG. 11. Effect of steam in the temperature dependence of coke deposition on Ni10AC. P_{CPA} = 26 kPa, P_{H_2} = 46 kPa, P_{N_2} or P_{H_2O} = 27 kPa.

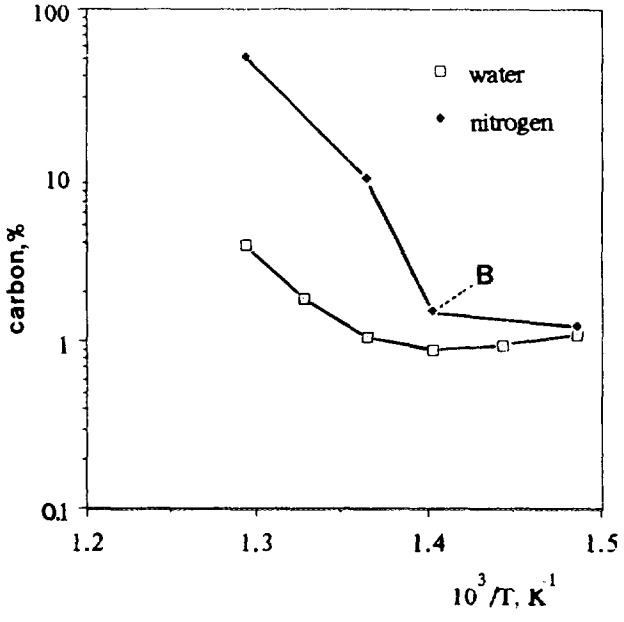

FIG. 12. Effect of steam in the temperature dependence of coke deposition on Ni10K4AC. P_{CPA} = 26 kPa, P_{H_2} = 46 kPa, P_{N_2} or P_{H_2O} = 27 kPa.

tal amount of carbon oxides produced by steam reforming remained practically unchanged (17).

DISCUSSION

Effect of Potassium on Hydrogen Chemisorption

In the present study we have found that the presence of increasing amounts of potassium in Ni/Al_2O_3 catalysts significantly enhances the volume of hydrogen which can be adsorbed. By contrast, no influence of alkali on the degree of reduction was observed. It was previously reported that, at the low pressures occurring in pulsed chromatography, the surface stoichiometry $H:Ni_S$ is lower than 1, and a value of 0.5 has proved to be in good agreement with both static volumetry and magnetic methods (9). This would lead in our case to mean dispersion values that increase with potassium content. However, the constant stoichiometry assumption may not stand with Ni–K catalysts. As an example, Praliaud *et al.* (*18*) have observed a decrease of both adsorbed volume and surface stoichiometry on K-addition to Ni/SiO_2 catalysts (1.1 to 0.6 for 0% to 2.7% K). Undoubtedly, the distribution of alkali between the nickel and the support will affect these parameters. With an inert support like silica, a definite amount of potassium was found in association with nickel and located predominantly at the surface of the particles (19). As a result, the chemisorption of H_2 and CO was reduced. Indeed, a greater effect is expected for smaller ions, such as sodium, which can be incorporated in the NiO lattice (20). However, a different kind of support or preparation method could reverse the

TABLE 5

Product Selectivities in the Competitive Reaction of Cyclopentane with Hydrogen and Water

Catalyst	*T*, °C	Conversion %	$\langle S_C \rangle$ %	$\langle S_H \rangle$ %	$\langle S_O \rangle$ %
Ni10AC	420	40	0.45	83.5	16
	440	34	0.59	81.4	18
	500	100	10.1	73.9	16
Ni10K4AC	420	57	0.30	80.7	19
	440	55	0.32	80.7	19
	500	68	1.2	73.8	25

Note. H_2/CPA = 1.75, H_2O/CPA = 1.04.

effect. Moore and Lunsford (6) reported that the addition of 2% K to Ni/ZrO_2 increases 2.2-fold the hydrogen chemisorption. As far as alumina is concerned, Bailey *et al.*, (21) have concluded from TPR/TPD experiments that on Ni/Al_2O_3 catalysts most of the potassium is on the alumina. This should minimize the effect on exposed nickel, at least, to a maximum limiting potassium content. Furthermore, it is generally believed that supported metals prepared by sequential impregnation result in a poor association of the alkali with the active metal (22, 23). Higher dispersion values normally mean lower particle size. Yet, from XRD analysis, the same mean particle size results for catalysts with different K loadings (17). Therefore, potassium appears to promote hydrogen chemisorption (the H/Ni_S ratio being closer to unity than on unpromoted catalysts) without significantly changing the nickel particle size.

Effect of K on Coke Oxidation

TPO experiments for the reaction at 420°C showed that the alkali facilitates a gradual development of new carbon species, as the carbon deposit became more important. Furthermore, if the K loading is optimum, whisker-like carbon is formed (Fig. 5). At 460°C, however, more than one kind of carbon appears on the unpromoted catalyst. Such species are characteristic of Ni/Al_2O_3 catalysts, and have been associated with carbon on or dissolved in, nickel (T_p = 360–400°C), and with filamentary carbon (T_p = 600–650°C) (8, 14). At low content, the effect of potassium is clearly to promote the growing of the latter carbon type, which readily masks the low-temperature and intermediate species. Hence, we conclude that promotion with relatively low doses of potassium acts basically on the production of carbon filaments. The TPO profiles have also shown that the alkali catalyzes more and more the combustion of filamentary carbon, even though the total amount of carbon may grow (Fig. 4). A cooperative effect between Ni and K was also observed by Carrazza *et al.* (24). This is not the case for the intermediate carbon types formed upon reaction at 420°C (Fig. 2).

Effect of K on the Mechanism of Formation of Carbon Filaments

Potassium operates at definite stages of the mechanisms governing the formation of carbon deposits. Let us consider both the effect of temperature and potassium content in terms of the mechanism generally proposed for filamentary carbon formation, which includes (14, 15, 25):

(1) dissociation of the hydrocarbon on the nickel surface to give carbon atoms or carbidic carbon;

(2) dissolution of carbon in nickel and bulk and/or surface diffusion;

(3) reconstruction of the nickel crystallite with segregation of distorted graphite at the rear of the particle, the nickel particle becoming detached from the support matrix by the growing filament.

In the first stage it is normally assumed that the hydrocarbon is chemisorbed on a dual nickel site followed by successive α-scission of the C–C bonds (26):

$$C_nH_m + 2\ Ni_c \rightarrow C_nH_z\text{—}Ni_{2c} + \frac{(m-z)}{2} H_2 \qquad [1]$$

$$C_nH_z\text{—}Ni_{2c} + Ni_d \rightarrow C_{n-1}H_z' - Ni_{2c} + CH_x - Ni_d, \text{ etc.} \qquad [2]$$

However, in the case of cyclic hydrocarbons, and particularly cyclopentane, multiple scission of the C–C bonds takes place due to the instability of the five-carbon ring (27). Such a process could still occur in the presence of small amounts of potassium. Hence, hydrocarbon adsorption and hydrocracking steps are for this alkane better described by

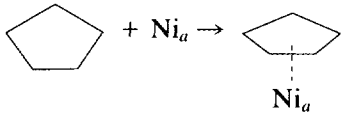

[3]

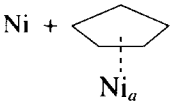

$$\rightarrow 5\ CH_X\text{—}Ni_d + (10\text{-}5x)/2\ H_2 \qquad [4]$$

where Ni_d designates an ensemble of d adjacent nickel atoms. The successive CPA dehydrogenation steps leading to coke via polymerization of adsorbed cyclodiolefins, a major path of coke formation on platinum catalysts (28), were omitted since bare Ni/Al_2O_3 catalysts yielded only small amounts of cycloolefins, and these are definitely suppressed upon K addition. Moreover, step [4] appears to be very fast compared to step [2] for linear hydrocarbons, which leaves $CH_x - Ni_d$ as the more abundant reaction intermediate. This species can react in two ways:

$$CH_x\text{—}Ni_d \rightarrow [Ni,C] \rightarrow C + d\ Ni + \frac{x}{2} H_2 \qquad [5]$$

$$CH_x\text{—}Ni_d + (2 - \frac{x}{2})\ H_2 \rightarrow CH_4 + d\ Ni. \qquad [6]$$

An additional step representing acid polymerization of the adsorbed fragment on adjacent alumina sites would only have some relevance on K-free catalysts in the presence of unsaturated residues. Steps [5] and [6] involve

either breaking or creation of C—H bonds, and could hardly be favored by alkali (29). However, it is not unlikely, under the low H_2/CPA ratio used in these experiments, that a fully dehydrogenating adsorption ($x = 0$ Eq. [4]) resulted in the formation of carbidic species (30). It has been reported that the reactivity of carbidic carbon with hydrogen on Ni, as well as on Fe and Co, is reduced in the presence of potassium (31). Nevertheless, a preferential formation of C–C at the expense of C–H bonds is not apparent from these results (Tables 3 and 4). Up to 1% K, the alkali accelerates *both* the hydrogenolysis reaction *and* the deposition of carbon, which means that reactions [5] and [6] proceed in parallel. By contrast, for higher K contents than 2%, the formation of carbon is the more affected.

The attachment of K to the catalysts after reduction at 500°C strongly suggests that it is in the ionic state (2). The formation of a complex K–O–Ni with electron-donating character, for which some evidence exists on Ni/SiO_2 (18), appears improbable on alumina-supported catalysts (21). Furthermore, any electron-enriched surface is expected to discourage both hydrogen and hydrocarbon dissociation, thus preventing carbon formation. Therefore, these assumptions cannot be invoked to explain the promotion of coking and hydrogenolysis at low K/Ni ratios. On the other hand, higher doses of K ions have been shown to have a large deactivating effect in the hydrogenation of benzene and in cyclopentane hydrogenolysis (12), presumably by affecting both hydrocarbon adsorption and hydrogenation of fragments. Hence, we believe that potassium, especially at high concentrations, would have a net retarding effect at this stage of the mechanism of filamentary carbon formation.

The role of alkali in the second stage appears, however, to be more limited. In fact, potassium could facilitate only the diffusion of carbon on the surface of the nickel crystallites (as it cannot be dissolved into them (32), thereby accelerating the steady-state filament growth rate. However, STEM combined with EDX analysis performed throughout the nickel particle at the tip of the carbon filament did not show any traces of potassium. Moreover, the formation of a carbonate phase stable under reaction conditions would introduce an additional resistance for carbon transport. Therefore, this stage also does not account for the enhancing of carbon deposition observed at low K-contents.

The third stage appears to be the most dependent on the Ni-support interaction. Far from hindering the nucleation of carbon filaments, the presence of relatively small amounts of potassium facilitates this process. The promoting action of alkali on the combustion of carbon filaments, as well as its appearance at the nickel–carbon interface, is linked to its high mobility. As potassium has a definite action on carbon formation without much affecting the nickel particle size (otherwise the nucleation stage could not be accomplished (15)), it must be located at the interstitial area between nickel and alumina forming a kind of potassium aluminate adlayer–Ni interface. A smaller contact angle between the nickel particle and the K-enriched peripheral support results, and the nickel–alumina interaction is weakened as a consequence. The "ability" to produce a filament is thus extended to smaller crystallites, which in the absence of alkali would become encapsulated on the surface (13, 15), and carbon grows more abundantly. This could explain the gradual appearance of thin filaments on Ni10K2AC after reaction at only 420°C, as well as the more intensively filamentary growth with increasing K content at 460°C. For higher K/Ni ratios, deactivation probably takes place by site blocking of the Ni ensembles by K adatoms (26). However, as Figs. 8 and 9 show, such a loss of catalytic activity has little influence on the temperature at which the carbon filaments begin to appear (B-point) (8). A lower value of the C/Ni_S ratio at this point (3.5–5 compared to 8–9 for Ni/Al_2O_3 catalysts) is now required for nucleation of the filament, which is consistent with a promotion by potassium of the nucleation step.

In summary, potassium would have antagonistic effects on stages (1) and (3); that is, the formation of surface carbon is definitely inhibited at high K/Ni ratios, while the restructuring and detachment of the Ni particle giving rise to carbon filaments is favored on small amounts of alkali addition. As a result, a maximum in the net rate of carbon deposition is observed.

Role of Potassium in the Presence of Water

On unpromoted catalysts, substitution of nitrogen by steam decreased the carbon deposition rates, while the production of filaments was practically unaffected. The decrease of the coking rate on steam addition has been explained in terms of a shorter residence time of the hydrocarbon fragments to form coke precursors when steam is present (26). In our case, this could explain the reduced carbon deposition observed at low temperatures. By contrast, the formation of filamentary carbon under these particular conditions was not affected by steam. On the other hand, when both steam and alkali are present, the absence of a sudden change in the apparent activation energy is in line with the scarce production of carbon filaments. Two roles of alkali have been generally invoked to account for coking inhibition in steam reforming (1, 2, 26): neutralization of the acidic support sites active for cracking, and promotion of the reaction between carbon and steam. Our results suggest that the first effect could prevent low temperature coke deposits, while the second should control the filament growth rate (24). Un-

doubtedly, additional experimental work under different operating conditions is needed to clarify these points.

CONCLUSIONS

In this study it has been found that the role of potassium ions on the hydrogenolysis and coking of Ni/Al_2O_3 catalysts is at least threefold:

(1) modifier of the metal–support interaction, as it reduces the adhesion strength between the nickel particles and the alumina matrix, which activates the formation of carbon filaments from these particles;

(2) basic agent, as it neutralizes the acidic sites of alumina necessary for the generation of coke precursors, whereby deactivation of the smaller nickel crystallites does not occur;

(3) inhibitor of hydrogenolysis and coking, since when present at high K/Ni ratios potassium appears to block specific sites for these reactions.

Furthermore, the alkali appears to promote the catalytic oxidation of filamentary carbon, without having much effect on the combustion of bidimensional carbon and coke. This would be in relation to the specific localization of the alkali between the nickel particle and the carbon tube of the filaments. Finally, potassium seems to favor hydrogen chemisorption on nickel, or the spillover of H atoms to the support, rather than to affect the metal particle size.

ACKNOWLEDGMENTS

This study was performed in the framework of an International Programme of Scientific Cooperation (PICS) sponsored by the CNRS and the CONICET, and both are gratefully acknowledged.

REFERENCES

1. Andrew, S. P. S., *Ind. Eng. Chem. Prod. Res. Dev.* **8,** 321 (1969).
2. Bridger, C. W., *Oil Gas J.*, 73 (Feb 16, 1976).
3. Mross, W. D., *Catal. Rev. Sci. Eng.* **25,** 591 (1983).
4. Figueiredo, J. L., and Trimm, D. L., *J. Appl. Chem. Biotechnol.* **28,** 611 (1978).
5. Chen, I., and Chen, F. L., *Ind. Eng. Chem. Res.* **29,** 534 (1990).
6. Moore, S. E., and Lunsford, J. H., *J. Catal.*, **77,** 297 (1982).
7. Huttinger, K. J., and Minges, R., *Fuel* **65,** 1122 (1986).
8. Duprez, D., Demicheli, M. C., Marecot, P., Barbier, J., Ferretti, O. A., and Ponzi, E. N., *J. Catal.* **124,** 324 (1990).
9. Duprez, D., Mendez, M., and Dalmon, J. A., *Appl. Catal.* **21,** 1 (1986).
10. Barbier, J., Churin, J., Parera, J. M., and Rivière, J., *React. Kinet. Catal. Lett.* **28,** 245 (1985).
11. Dexpert, H., Gallezot, P., and Leclercq, C., *in* "Les Techniques Physiques d'Etudes des Catalyseurs "(B. Imelik and J. C. Védrine, Eds.), p. 676. Technip, Paris, 1988.
12. Duprez, D., Demicheli, M. C., Marecot, P., Barbier, J., Ferretti, O. A., and Ponzi, E. N., *Stud. Surf. Sci. Catal.* **68,** 195 (1991).
13. Baker, R. T. K., *in* "Chemistry and Physics of Carbon" (P. L. Walker, Jr. and P. A. Thrower, Eds.), Vol. 14, p. 83. Dekker, New York, 1978.
14. Bartholomew, C. H., *Catal. Rev. Sci. Eng.* **24,** 67 (1982).
15. Figueiredo, J. L., *in* "Progress in Catalyst Deactivation," NATO Advanced Study Institute Series, Series E, Vol. 54, p. 45. Kluwer, Dordrecht, 1981.
16. Yang, R. T., and Chen, J. P., *J. Catal.* **115,** 52 (1989).
17. Demicheli, M. C., Thesis. Poitiers, 1991.
18. Praliaud, H., Primet, M., and Martin, G. A., *Appl. Surf. Sci.* **17,** 107 (1983).
19. Pitchon, V., Gallezot, P., Nicot, P., and Praliaud, H., *Appl. Catal.* **47,** 357 (1989).
20. El-Shobaky, G. A., and Petro, N. S., *Surf. Technol.* **13,** 197 (1981).
21. Bailey, K. M., Campbell, T. K., and Falconer, J. L., *Appl. Catal.* **54,** 159 (1989).
22. Kesraoui, S., Oukaci, R., and Blackmond, D. G., *J. Catal.* **105,** 432 (1987).
23. Hoost, T. E., and Goodwin, J. G., Jr., *J. Catal.* **130,** 283 (1991).
24. Carrazza, J., Chludzinsky, J. J., Jr., Heinemann, H., Somorjai, G. A., and Baker, R. T. K., *J. Catal.* **110,** 74 (1988).
25. Rostrup-Nielsen, J. R., and Trimm, D. L., *J. Catal.* **48,** 155 (1977).
26. Rostrup-Nielsen, J. R., "Steam Reforming Catalysts." Danish Technical Press, Copenhagen, 1975.
27. Matsumoto, H., Saito, I., and Yoneda, Y., *J. Catal.* **19,** 101 (1970).
28. Barbier, J., *Appl. Catal.* **23,** 225 (1986).
29. Zaera, F., and Somorjai, G. A., *J. Catal.* **84,** 375 (1983).
30. Leach, H. F., Mirodatos, C., and Whan, D. A., *J. Catal.* **63,** 138 (1980).
31. Campbell, C. T., *Adv. Catal.* **36,** 1 (1989).
32. Hansen, M., "Constitution of Binary Alloys." McGraw–Hill, New York, 1958.